Phase Behavior of the Restricted Primitive Model and Square-Well Fluids from Monte Carlo Simulations in the Grand Canonical Ensemble

Gerassimos Orkoulas and Athanassios Z. Panagiotopoulos*

School of Chemical Engineering, Cornell University, Ithaca, NY 14853-5201

and

Institute for Physical Science and Technology and Department of Chemical Engineering, University of Maryland, College Park, MD 20742-2431

ABSTRACT

Coexistence curves of square-well fluids with variable interaction width and of the restricted primitive model for ionic solutions have been investigated by means of grand canonical Monte Carlo simulations aided by histogram reweighting and multicanonical sampling techniques. It is demonstrated that this approach results in efficient data collection. The shape of the coexistence curve of the square-well fluid with short potential range is nearly cubic. In contrast, for a system with a longer potential range, the coexistence curve closely resembles a parabola, except near the critical point. The critical compressibility factor for the square-well fluids increases with increasing range. The critical behavior of the restricted primitive model was found to be consistent with the Ising universality class. The critical temperature was obtained as T_c=0.0490±0.0003 and the critical density ρ_c=0.070±0.005, both in reduced units. The critical temperature estimate is consistent with the recent calculation of Caillol *et al.* [*J. Chem. Phys.*, **107**, 1565, 1997] on a hypersphere, while the critical density is slightly lower. Other previous simulations have overestimated the critical temperature of this ionic fluid due to their failure to account for finite-size effects in the critical region. The critical compressibility factor ($Z_c=P_c/\rho_c T_c$) for the ionic fluid was obtained as Z_c=0.024±0.004, an order of magnitude lower than for non-ionic fluids.

Revised version submitted to *J. Chem. Phys.*, Oct. 7, 1998; 21 pages +10 figures

*Author to whom correspondence should be addressed at the University of Maryland.
E-mail: thanos@ipst.umd.edu

I. INTRODUCTION

Significant methodological progress has been made over the years in the development of Monte Carlo algorithms capable of predicting phase equilibrium properties for model systems[1,2,3,4]. A commonly used simulation method is the Gibbs Ensemble Monte Carlo method of Panagiotopoulos[1]. This method utilizes two physically detached but thermodynamically connected boxes representative of the coexisting phases. Particle transfers and volume exchanges between the boxes lead to establishment of phase equilibrium.

The Gibbs ensemble method provides information at a single temperature for which the simulation was performed. The calculations must be repeated at different temperatures in order to cover the entire coexistence range, which is, in principle, a tedious and time consuming process. An alternative technique by Ferrenberg and Swendsen[5] has potentially higher efficiency by increasing the amount of information that can be obtained from a *single* simulation. This is achieved by forming histograms of fluctuating observables during the course of the simulation. These histograms provide the means of calculating thermodynamic properties of the state under investigation as well as of neighboring states. The latter can be achieved by extrapolating (reweighting) the histogram of the reference state. This histogram reweighting procedure is particularly useful in the critical region where, owing to the large fluctuations, a single simulation covers wide ranges of the associated parameter space.

All molecular simulation techniques encounter difficulties in the critical region since they utilize finite systems and cannot capture the divergence of the correlation length. Finite-size scaling techniques, however, afford accurate estimates of infinite-volume critical points from simulations of systems of finite size. These methodologies have mainly been applied to lattice-based magnetic systems[6,7,8,9] but they have recently been extended to off-lattice fluids by explicitly accounting for the lack of symmetry between the coexisting phases[10]. These theories are based on the observation that, at criticality, the distribution functions of certain fluctuating observables assume universal and scale invariant forms. These universal (also known as scaling) functions are the same for every fluid in a given universality class. This fact can be utilized to obtain accurate estimates of critical points, provided that these functions are independently known.

In this work, we have carried out grand canonical Monte Carlo simulations aided by histogram reweighting, multicanonical sampling and finite-size scaling techniques to obtain the

coexistence curves and the associated critical points of square-well fluids and of the restricted primitive model. We begin by defining the model potentials and we also give some necessary details on the methods used. We then present results for the systems studied and comparisons with previous data and finally conclude by discussing potential advantages, possible drawbacks and future applications of the computational methods used in this work.

II. MODELS STUDIED

Systems interacting according to square-well (SW) potentials have been studied extensively,[11,12,13,14,15] since they constitute the simplest off-lattice fluids that exhibit phase separation. The pair potential between particles i and j, separated by a distance r_{ij}, is defined by

$$U_{ij}=\begin{cases}\infty & r_{ij}\le\sigma\\ -\varepsilon & \sigma<r_{ij}\le\lambda\sigma\\ 0 & r_{ij}>\lambda\sigma\end{cases} \qquad (1)$$

where ε and λ are the interaction range and strength respectively. As is common in simulations, appropriate reduced quantities (temperature T^* and density ρ^*) can be defined by scaling with the energy parameter ε, and the particle diameter σ, e.g. $T^*=k_BT/\varepsilon$ and $\rho^*=\rho\sigma^3$ where k_B is Boltzmann's constant (k_B=1.381·10^{-23}J/K). In the remainder of this paper, we omit asterisks from reduced quantities for the sake of simplicity. Knowledge of the phase behavior is of considerable theoretical importance since by varying the interaction range, λ, this model can interpolate between the hard-sphere and the long-range van der Waals fluid.

The restricted primitive model (RPM) consists of a collection of hard spheres of equal diameter σ, half of them carrying positive charge and the other half negative that interact via a Coulomb potential. The charged spheres are allowed to move in a structureless background characterized by dielectric constant D. In accordance with Coulomb's law the pair potential is taken to be

$$U_{ij} = \begin{cases}\dfrac{1}{4\pi DD_0}\dfrac{z_i z_j e^2}{r_{ij}} & r_{ij}\ge\sigma\\ \infty & r_{ij}<\sigma\end{cases} \qquad (2)$$

where z_ie and z_je are the charges of ions i and j respectively ($|z_i|=|z_j|$), e is the charge of the electron (e=1.602·10^{-19}C), D is the dielectric constant of the medium and D_0 is the dielectric

permeability of the vacuum (D_0=8.85·10^{-12}C^{2}N^{-1}m^{-2}). Reduced temperature and density are defined by scaling with the Coulomb energy between two ions at contact, $e^2/4\pi DD_0\sigma$, and the size parameter, σ.

There have been numerous theoretical[16] and numerical[17] attempts aimed on establishing the RPM coexistence curve and associated critical point. Despite these efforts, there are still significant disagreements among results of different investigations. One of the reasons for these differences is the strong Coulomb force that causes the system to associate and renders both theoretical and numerical investigations of the system significantly harder than corresponding non-ionic fluids. Recent Monte Carlo simulations[18,19,20] as well as theoretical advances[21,22] have resulted in estimates for T_c≈0.055 and ρ_c≈0.03-0.05, although there is considerable scatter among results from different investigations. The question of the universality class to which this model belongs still remains open. For fluids for which ionic species are present, one generally distinguishes between solvophobic and Coulombic phase separation[23]. Solvophobic phase separation is driven primarily by the short-range solvent-salt or vacuum-salt interactions, whereas Coulombic phase separation is driven be the strong electrostatic forces. Experimental studies of ionic fluids have found Ising behavior[24,25] in some systems, classical mean-field[26,27] in others and crossover behavior in yet other systems[28,29]. Recent experiments, however, do not seem to support the classical or even crossover scenario from classical to Ising behavior[30,31].

III. SIMULATION METHODOLOGIES

A. Histogram reweighting and multicanonical sampling

The idea of sorting the simulation data in the form of histograms of fluctuating observables in order to obtain properties of the state under investigation and neighboring states is quite old[32]. It had not been used in investigations of subcritical and near-critical coexistence properties of fluids until the work of Ferrenberg and Swendsen[5] for lattice-based magnetic systems. In a grand canonical Monte Carlo simulation at fixed chemical potential μ_0, temperature T_0 (or inverse temperature K_0=1/k_BT_0), and volume V (or linear size L=$V^{1/3}$), the joint probability of observing a given number of particles N (or density ρ=N/V) and energy E is

$$f_0(N,E) \quad = \quad W(N,V,E)\exp\left(\mu_0 N - K_0 E + F_0\right) \qquad (3)$$

where the microcanonical partition function *W(N,V,E)*, which is related to the entropy, features as the density of states in this expression and

$$F_0 \;=\; F(\mu_0,V,T_0) \;=\; -\ln\left\{\sum_N\sum_E W(N,V,E)\exp(\mu_0 N - K_0 E)\right\} \qquad (4)$$

is the grand canonical free energy (pressure) of the simulated state. The joint distribution of energy and density can be readily obtained as a two-dimensional histogram in the course of the grand canonical simulation. The information stored in the form of a histogram can be used to obtain the probability distribution at a different state point (μ, T) since, in view of Eq. (3) one can write

$$f(N,E) \;=\; W(N,V,E)\exp(\mu N - KE + F) \qquad (5)$$

and by eliminating W using Eqs. (3) and (4)

$$f(N,E) \;=\; \frac{f_0(N,E)\exp\left[(\mu-\mu_0)N-(K-K_0)E\right]}{\sum_N\sum_E f_0(N,E)\exp\left[(\mu-\mu_0)N-(K-K_0)E\right]} \qquad (6)$$

In practice, the extrapolation implied by Eq. (6) only works if $|\mu\text{-}\mu_0|$ and $|T\text{-}T_0|$ are not too large. Otherwise the bulk of the weight of the new histogram, *f(N,E)*, comes from the tail of the original histogram, $f_0(N,E)$, and hence will have poor statistics. In order to cover wider ranges one can perform several Monte Carlo runs that correspond to different but overlapping N and E ranges and then match the entropy function in the neighborhood region where the histograms provide data. An efficient way of combining the histograms from several simulations has been proposed by Ferrenberg and Swendsen[33]. For r Monte Carlo runs, the optimum density of states function that minimizes the difference between observed and predicted histograms, is given by

$$W(N,V,E) \;=\; \frac{\sum_{i=1}^{r} H_i(N,E)}{\sum_{i=1}^{r} h_i \exp(\mu_i N - K_i E + F_i)} \qquad (7)$$

where $H_i(N,E)$ and h_i are the number of *(N, E)* and total observations respectively for the i-th run (i=1,2,···,r). The free energy, F_i, of state i, must be evaluated self-consistently from

$$\exp(-F_i) \;=\; \sum_N\sum_E W(N,V,E)\exp(\mu_i N - K_i E) \qquad (8)$$

In the context of investigating phase transitions through histogram reweighting Ferrenberg and Swendsen[5] recommend performing simulations in the near-critical region. This is because the histograms obtained are broad due to the large fluctuations that characterize the neighborhood of the critical point. It is well known[34,35] that the grand canonical density distribution associated with subcritical temperatures and near-coexistence chemical potentials, attains a characteristic double-peaked structure. The two peaks are associated with stable (or metastable) phases whereas the minimum between them can be attributed to the formation of interfaces[36].

Far below the critical point, a conventional grand canonical simulation will thus encounter serious ergodicity problems due to the size of the barrier that separates the two bulk phases. The multicanonical ensemble approach[37], however, overcomes these difficulties by artificially enhancing the otherwise infrequent transitions between the bulk phases. The improvement is achieved by sampling not from the physical density distribution, $f(\rho) \propto \exp(\mu\rho V)$, but from a modified one, $\pi(\rho)$, that is nearly-flat throughout the entire region. The modified distribution, $\pi(\rho)$, is related to the physical one, $f(\rho)$, through a weight function $g(\rho)$

$$\pi(\rho) = g(\rho) \cdot f(\rho) \tag{9}$$

It is apparent that the choice $g(\rho)=1/f(\rho)$ will result in uniform sampling throughout the density range targeted for study. One clearly needs a prior estimate of the density distribution $f(\rho)$ in order to use it as a preweigthing function. This estimate, however, can be readily obtained from histogram reweigthing of a near-critical density distribution. The latter can be easily obtained since the barrier associated to the formation of interfaces is small in the critical region. Once uniform sampling has been achieved, the improved grand canonical density histogram, $f(\rho)$, can be obtained from the measured one, $\pi(\rho)$, by dividing out the preweighting function $g(\rho)$

$$f(\rho) = \pi(\rho) \Big/ g(\rho) \tag{10}$$

This procedure can then be repeated by extrapolating the improved density distribution at even lower temperatures and using its inverse as a new weight function. Closely related to the multicanonical ensemble technique are the methods of entropic sampling[38], expanded ensembles[39] and simulated tempering[40].

B. Finite-Size Scaling

In the critical region, the correlation length ξ grows very large and often exceeds the linear size L of the finite system. For such a case, the singularities and discontinuities that characterize critical behavior in the thermodynamic limit are smeared out and shifted. The infinite-volume critical point of a system can, however, be extracted from finite systems by examining the size dependence of certain thermodynamic observables. Fisher and coworkers first developed this methodology which is known as finite-size scaling[41].

The finite-size scaling approach that has been used in this work is the one proposed by Bruce and Wilding[10] that accounts for the lack of symmetry between the coexisting phases. Due to the absence of particle-hole symmetry, the scaling fields comprise linear combinations of the coupling $K=1/k_BT$ and chemical potential differences[42]

$$\begin{aligned} \tau &= K_c - K + s\left(\mu - \mu_c\right) \\ h &= \mu - \mu_c + r\left(K_c - K\right) \end{aligned} \qquad (11)$$

where τ is the thermal scaling field and h is the ordering scaling field. The subscript c signifies value at criticality. Parameters s and r are system specific quantities that control the degree of field mixing. r is the limiting critical gradient of the coexistence curve in the μ-K plane[42]. On the other hand, s controls the degree at which the chemical potential features in the thermal scaling field τ.[42] This field mixing effect is manifested in the widely observed singularity of the coexistence curve diameter of fluids.[43,44,45]

Associated with these scaling fields are the scaling operators M and E that are found[10] to comprise linear combinations of the particle density ρ and the energy density $u=E/V$,

$$\begin{aligned} M &= \frac{1}{1-sr}\left(\rho - s\,u\right) \\ E &= \frac{1}{1-sr}\left(u - r\,\rho\right) \end{aligned} \qquad (12)$$

For systems possessing the symmetry of the Ising model, M is simply the magnetization whereas E is the energy density. General finite-size scaling arguments[10,36,46] predict that at criticality the probability distributions $P_L(M)$ and $P_L(E)$ exhibit scaling behavior of the form

$$\begin{aligned} P_L(M) &= A\,L^{\beta/\nu}\,P_M^*\left(A\,L^{\beta/\nu}\,\delta M\right) \\ P_L(E) &= B\,L^{(1-\alpha)/\nu}\,P_E^*\left(B\,L^{(1-\alpha)/\nu}\,\delta E\right) \end{aligned} \qquad (13)$$

where α, β, and ν are the standard critical point exponents. δM and δE signify deviations from criticality ie. $\delta M = M - M_c$. The functions P_M^* and P_E^* are universal, i.e., the same for every fluid in a given universality class while A and B are non-universal (system specific) constants.

For the Ising universality class, these scaling functions can be readily obtained as histograms by Monte Carlo simulation at the known critical point of the Ising model[47]. Analytical approximations have also become available recently[48]. In order to estimate the critical point of a fluid of the Ising class one can obtain the distribution $P_L(M)$ and then (through histogram reweighting) search for the point for which $P_L(M)$ collapses onto P_M^*.

IV. THE PHASE BEHAVIOR OF SQUARE-WELL FLUIDS

We have studied the coexistence region of the square-well fluids with interaction range, λ, of 1.5 and 3, by performing grand canonical Monte Carlo simulations aided by histogram reweighting and finite-size scaling techniques. The simulations were implemented according to the algorithm of Norman and Filinov[49]. For each case, six linear sizes were utilized: L=6, 8, 10, 12, 15 and 18σ. In order to facilitate computations, the simulation volume, $V=L^3$, was partitioned into cubic cells of size $\lambda\sigma$. This approach ensures that the interactions of the particles at a given cell extend at most to the 26 neighboring cells. The observables recorded were the density, ρ, the energy density, u, and the histogram of the joint distribution $f(\rho,u)$. The length of the runs was $50\text{-}300\cdot10^6$ configurations depending of the system size and the density range covered. Particle transfers were attempted with frequency 90% (45% insertions and 45% removals respectively) and particle displacements with frequency 10%.

In order to initiate the investigations, we performed a series of very short runs for the smaller system sizes (L=6 and 8σ). In these runs, the temperature and chemical potential were tuned until the density distribution $f(\rho)=\int f(\rho,u)\mathrm{d}u$ exhibited a double peaked structure with a shallow minimum. A longer run was then performed in order to accumulate better statistics. To obtain the critical point, we utilized the matching condition of the order parameter probability distribution $P_L(M)$ onto its limiting form P_M^*. The histogram of $P_L(M)$ was obtained from $f(\rho,u)$ using $M=\rho-su$ and integrating over the energy fluctuations. The process was repeated (by changing T, μ, and s through histogram reweighting) until satisfactory collapse onto P_M^* was obtained. The result of applying this procedure for the square-well fluid with λ=1.5 and L=8σ is

shown in Fig. 1. The estimates for the critical temperature and chemical potential for this system size were $T_c(L)$=1.220, $\mu_c(L)$=-2.9518.

Using the small-L critical point estimate we performed additional simulations for larger system sizes in order to implement finite-size scaling analysis. The critical parameters were found to be L-dependent because of corrections to scaling. Similar size dependence was also found by Wilding in the study of the Lennard-Jones fluid[50] that showed that it is possible to obtain an estimate of the infinite-volume critical point by including the leading correction-to-scaling exponent. The apparent critical temperature $T_c(L)$ deviates from the infinite-volume limit $T_c(\infty)$ as

$$T_c(L)-T_c(\infty)\propto L^{-(\theta+1)/\nu} \qquad (14)$$

where θ and ν are the correction-to-scaling and correlation length exponents respectively. Their values have been estimated to be $\theta\approx$0.54 and $\nu\approx$0.629 for the 3D Ising class[51,52]. The critical temperature of the infinite system can be determined from a least-squares fit. The critical density can also be obtained from scaling considerations. The L-dependent critical density, $\rho_c(L)$, obtained as the first moment of the density distribution at $\mu_c(L)$ and $T_c(L)$, is extrapolated to the thermodynamic limit according to[50]

$$\rho_c(L)-\rho_c(\infty)\propto L^{-(1-\alpha)/\nu} \qquad (15)$$

where $\alpha(\approx 0.11)$[51,52] is the exponent associated with the divergence of the heat capacity. The dependence of the critical point parameters on the linear system dimension is shown in Fig. 2 for the square-well fluid with λ=3. The infinite-volume critical point parameters are obtained by a least-squares fit. Our results for the critical point parameters extrapolated to the limit of infinite system size are summarized in Table I.

In order to obtain subcritical coexistence information, we utilized the near-critical coexistence simulations augmented with additional runs for very low and high densities in order to improve statistics and cover even wider ranges of the associated parameter space (μ and T). For very low temperatures a few multicanonical simulations were also employed according to the procedure outlined in the previous section. The weight (or bias) function $g(\rho)$ that was used in the multicanonical simulations was obtained from the near-critical density distributions by histogram reweighting.

Our results for the coexistence densities of the square-well fluids are given in Figs. 3 and 4. The equal weight construction[53] was used to obtain the coexistence chemical potential for a given temperature. Saturated vapor and liquid densities were determined from the first moment under each peak of the density distribution that corresponds to coexistence. The large number of points obtained is a consequence of the histogram reweighting. The combination of data in one histogram, the subsequent reweighting, and the coexistence point location constitute a minute faction of the total computational effort. One can then obtain information for a large number of thermodynamic states, as is apparent in Figs. 3 and 4, at little extra cost. In the framework of the histogram reweighting scheme, it is also more convenient to utilize small system sizes in order to extrapolate over wide regions of the associated parameter space. As Figs. 3 and 4 indicate, for T not to close to T_c, the coexisting densities are practically independent on the system size L.

In Fig. 3, our grand canonical data for λ=1.5 are compared with the results of Vega *et al.*[12] which were obtained by Gibbs ensemble Monte Carlo simulations. While the agreement is rather satisfactory, the grand canonical Monte Carlo results for the coexistence densities, appear to be more consistent than the scattered Gibbs ensemble data. The likely explanation is the quality of Monte Carlo sampling. A grand canonical simulation in the two-phase region samples the entire density domain with an average acceptance rate of 20-25% for the particle transfers. In contrast, the Gibbs ensemble random walk, which concentrates on sampling the region around the peaks of the density distribution, yields low acceptance rates (<5%)[1] for particle transfers between the coexisting phases. Due to the coupling of the two simulation boxes in the Gibbs methodology, trial moves that modify the number of particles or the volume must produce a favorable change in both boxes in order for the overall step to be accepted. The previous reasoning indicates that Monte Carlo sampling in the grand canonical ensemble is more efficient than in the Gibbs ensemble.

Recently, Brilliantov and Valleau[54] have performed a numerical study of the coexistence region of the short-ranged (λ=1.5) square-well fluid. They have used a computational technique known as density (or thermodynamic) scaling Monte Carlo[2]. Their estimate of the infinite-system size critical point, T_c≈1.22±0.01, is in agreement within simulation uncertainty with our estimate (T_c=1.2180±0.0003). The grand canonical Monte Carlo approach used in the present study allows for calculations involving larger system sizes and results in smaller statistical uncertainties for the infinite-system critical point parameters. In addition, the grand canonical

approach allows studies at highly subcritical temperatures, at which the difference in density between the coexisting phases hampers efficient sampling in density scaling Monte Carlo. Otherwise, equivalent thermodynamic property information is obtained from the two approaches.

To investigate the phase behavior of the square-well fluid with interaction range of λ=3, Benavides *et al.*[15] performed interfacial molecular dynamics simulations of a fluid confined between two parallel hard walls. While these interfacial simulations can provide valuable information about the vapor-liquid interface, they require a large number of particles in order to yield a stable interface and minimize the effect of confinement. The grand canonical simulations appear to provide more accurate results with much smaller system sizes, as is apparent in Fig. 4.

A point that merits special attention is the shape of the coexistence curves of the square-well fluids. The coexistence envelope of the square-well fluid with short-ranged intermolecular interaction is nearly cubic in shape, a point also emphasized by Vega *et al.*[14]. In contrast, the phase boundary of the square-well fluid with somewhat longer interaction width, appears to be parabolic in shape away from T_c. Its critical point, however, is expected to be of the Ising type, as for all systems with interactions of finite range and a scalar order parameter. This behavior implies a crossover from asymptotic Ising behavior to classical mean-field behavior away from the critical point. The primary factor for these crossover phenomena is the long range of the interactions which can suppress the long-range critical fluctuations. Similar crossover phenomena have also been seen in in simulation studies of two-dimensional spin systems with extended interaction ranges[55]. Theoretical attempts to investigate the nature of these phenomena in fluids and fluid mixtures have appeared recently[56,57].

The temperature dependence of the vapor pressure curve for these two fluids is given in Figs. 5 and 6. Simulation uncertainties are smaller than the symbol size. For a given temperature, the area under each peak of the coexistence density distribution was calculated and a quantity proportional to the partition function was thus obtained. The pressure, within an additive constant, was subsequently obtained from the partition function. The additive constant was estimated by considering a reference state of known pressure, the gas at very low density, which obeys the ideal gas law. Our results for the pressure of the of λ=1.5 system are consistent with those of Brilliantov and Valleau.[54] Results of Brilliantov and Valleau for N=256 shown in Fig. 5 were terminated at the infinite-system estimated critical temperature. The critical pressure listed in Table I was estimated as follows. The vapor pressure curve was plotted as ln(P) versus

$1/T$, which results in a nearly perfect straight line even near the critical point. The critical pressure was then obtained by extrapolation to the infinite-system critical temperature. The extrapolation distance is shown in Figs. 5 and 6 as the dotted line linking the points near the critical pressure. From the critical pressure, the critical compressibility factor, $Z_c = \frac{P_c}{\rho_c T_c}$, was obtained. The critical compressibility factor increases with λ, from Z_c=0.252 for λ=1.5 to Z_c=0.331 for λ=3. For comparison, i.e. for argon[63] Z_c=0.291, while the van der Waals equation of state predicts Z_c=0.375. As expected, the longer-range square-well fluid approaches the van der Waals value.

V. THE COEXISTENCE REGION OF THE RESTRICTED PRIMITIVE MODEL

While the critical behavior of fluids characterized by short-ranged intermolecular interactions is rather well understood, the situation is not clear for fluids for which electrostatic forces drive the phase transition. This section addresses the question of RPM criticality. In order to perform pair transfers efficiently in our grand canonical simulations, we implemented a distance-biased Monte Carlo move as in our previous work[19]. The summation of the slowly decaying Coulomb potential was done by the Ewald method[58] with vacuum boundary conditions at infinity. Four linear sizes were utilized: L=10, 12 13 and 14σ. The total length of the runs was 3-20$\cdot 10^8$ configurations, depending on the system size and density range investigated. Pair transfers were attempted with frequency 70% and single-ion displacements with frequency 30%. Acceptance rate of the transfers was 5-8% in the near-critical region.

In order to estimate the critical point, we implemented the matching of the order parameter distribution onto its Ising limiting form. The quality of the mapping, which is shown in Fig. 7, is not as good as in the case of the square-well fluids (cf. Fig. 1). It is evident from Fig. 7 that the number of ions is too small to allow for a well-defined low-density peak. Utilizing larger sizes would be computationally prohibitive. As in the case of the square-well fluids, we repeated this matching procedure for every system size studied and extrapolated the L-dependent critical temperature and density to the limit of infinite size according to Eqs. (14) and (15). This task is shown in Fig. 6. Our estimates of the critical point parameters for the restricted primitive model are summarized in Table I.

In Fig. 8, our results for the scaling of the RPM critical temperature and density with system size are compared to those of Caillol *et al.*,[59] also obtained by mixed-field finite-size scaling techniques. Their work was based on performing Monte Carlo simulations for an ionic fluid that consists of charged hard particles moving on the surface of a four-dimensional hypersphere[60]. The evaluation of the Coulomb potential on the hypersphere appears to be 3-4 times faster than the more traditional Ewald sum that was used in this work. Extrapolation of the apparent critical temperature $T_c(L)$ to the limit of infinite system size is shown in Fig. 8(a). The two sets of data seem to extrapolate at approximately the same infinite-volume critical temperature, even though they approach the thermodynamic limit with different slope. In near-critical finite systems, the geometry and nature of the boundaries play an important role[41,61] and this causes $T_c(L)$ obtained on a hypersphere to be different than the one obtained for a three-dimensional periodic system. Nevertheless, if the two distinct finite systems are to be associated with a given physical system (the RPM is this case) they should correspond to the same critical point in the thermodynamic limit. On the other hand, the apparent critical densities for the two independent sets of data do not seem to extrapolate to the same infinite-volume limit, as Fig. 8(b) indicates. However, as Müller and Wilding point out[62], ρ_c cannot be determined as accurately as T_c or μ_c. In addition, no allowances for corrections to scaling were made in Eq. (15). Since the simulated system sizes were certainly small, corrections to scaling may turn out to be important for an accurate determination of ρ_c. Despite the difference in the estimate for ρ_c between our study and the study of Caillol *et al.*,[59] it is now clear that earlier estimates[18, 19, 20] of the RPM critical density were significantly below the value obtained from finite-size scaling methods. The likely reason for this discrepancy is discussed in the following paragraph.

The coexistence curve of the restricted primitive model from the present work is shown in Fig. 9. Our data do not extend much below the critical temperature due to difficulties associated with sampling for the ionic fluids. The new coexistence data are compared with the earlier results of Panagiotopoulos[18], Caillol[19] and Orkoulas and Panagiotopoulos[20] that were obtained from Gibbs ensemble simulations. While the agreement is reasonable for the subcritical coexistence region, the previous Gibbs ensemble studies overestimate the critical temperature by approximately 10%. This discrepancy can probably be attributed to analytic extensions of the coexistence curve associated with finite systems and supercritical temperatures. These extensions were falsely taken as evidence of true phase coexistence in all these studies and

consequently the critical temperature was overestimated. Because of the asymmetry of the RPM phase diagram and the resulting strong and negative slope of the coexistence curve diameter, an overestimation of T_c also results in an underestimation of $\rho_{c.}$ This explains the difference in critical density between the present study and that of references[18-20]. The critical density of the RPM is now estimated to be approximately four times lower than that of simple non-polar fluids.

The vapor pressure curve for the RPM is shown in Fig. 10. Pressures were obtained by using as reference sufficiently low densities so that the system behaves as an ideal gas of dimers ($\rho \approx 10^{-4}$). At the temperatures of interest, the RPM does not behave as an ideal gas of single ions until much lower densities, not probed in our simulations. The critical compressibility factor obtained from our estimate of the critical pressure is Z_c=0.024, an order of magnitude lower than for the non-ionic fluids. The lowest value of Z_c in a compilation of experimental data for common gases and liquids[63] is Z_c=0.12 for HF, with most values for other fluids in the range Z_c=0.25 to 0.40.

VI. CONCLUSIONS

In this work, we have utilized histogram-based and finite-size scaling techniques to investigate the coexistence region of pure fluids by grand canonical Monte Carlo simulations. These methodologies appear to provide a simple and highly efficient route to phase coexistence calculations. The choice of the grand canonical ensemble was dictated by reasons of computational simplicity. Similar results could, in principle, be obtained through constant pressure (isothermal-isobaric) simulations. In such a case the density fluctuates by virtue of volume expansions and compressions and the reweighting procedure can be applied by recording histograms of molar volume. In addition, mixed-field finite size scaling techniques can also be applied to fluids at constant pressure conditions.[64] Constant pressure simulations might be efficient for systems for which their pair potential functions scale with the box length. For most fluids, however, trial volume moves are computationally expensive since they require a full energy recalculation, an O(N^2) operation. On the other hand, trial particle transfers in the grand canonical ensemble are not too demanding since the associated energy change constitutes an O(N) calculation.

It was confirmed from the finite-size scaling analysis that the critical points of the square-well fluids with finite interaction range are of the Ising type. However, certain crossover effects

in the shape of the coexistence curve are apparent (Fig. 4). The interaction range must, of course, play a significant role in the shape of the coexistence curve away from the critical point. The critical compressibility factor was found to increase with the interaction range in accord with theory.

In the absence of certainty about the nature of ionic criticality, we assumed that the primitive model of electrolytes also belongs to the Ising universality class. Our data are consistent with this hypothesis, but are not of sufficiently high accuracy and for a large enough range of system sizes to exclude other possibilities. Similar conclusions were reached by Caillol *et al.*[59] in their study of the primitive model on a hypersphere. On the other hand, recent simulation results by Valleau and Torrie[65] provide no indication of an Ising-type divergence of the heat capacity. Recent theoretical advances based on implementing the Ginzburg criterion[66] for the restricted primitive model have found[67,68,69,70] that this model should exhibit little (if any) non-Ising behavior. Clearly, this latest picture that neither supports mean-field behavior nor a crossover scenario contradicts several experimental observations. It is believed that charge oscillations may provide a second order parameter that competes with the density fluctuations[69]. This issue certainly deserves further theoretical and numerical study.

The critical temperature of the RPM was found to be T_c=0.0490±0.0003, lower than most previous investigations. Due to the slope of the coexistence curve diameter, the new, lower estimate for critical temperature also resulted in a significantly higher estimate for the critical density. The critical compressibility factor, $Z_c=P_c/\rho_c T_c$, for the RPM is Z_c=0.024±0.004, an order of magnitude lower than non-ionic fluids. The low value of the critical compressibility factor may serve as an indicator of true Coulombic criticality in experimental systems.

ACKNOWLEDGMENTS

The authors would like to thank Dr. N. B. Wilding for helpful discussions and for providing copies of papers prior to publication, and Prof. M. E. Fisher for detailed comments on a draft of the manuscript. GO would like to acknowledge the hospitality of Prof. D. N. Theodorou at the University of Patras, Greece, where this manuscript was prepared. Financial support for this work was provided by the Department of Energy, Office of Basic Energy Sciences, under contract DE-FG02-89ER141014. Supercomputing time was provided by the Cornell Theory Center.

REFERENCES

[1] A. Z. Panagiotopoulos, Molec. Phys. **61**, 813 (1987); Molecular Simulation **9**, 1 (1992).

[2] J. P. Valleau, J. Comp. Phys. **96**, 193 (1991).

[3] D. A. Kofke, Molec. Phys. **78**, 1331 (1993); J. Chem. Phys. **98**, 4149 (1993).

[4] A. Lotfi, J. Vrabec, and J. Fischer, Molec. Phys., **76**, 1319 (1992).

[5] A. M. Ferrenberg and R. H. Swendsen, Phys. Rev. Lett. **61**, 2635 (1988).

[6] *Finite Size Scaling and Numerical Simulation of Statistical Systems*, edited by V. Privman (World Scientific, Singapore, 1990).

[7] A. M. Ferrenberg, and D. P. Landau, Phys. Rev. B **44**, 5081 (1991).

[8] K. Binder, in *Computational Methods in Field Theory*, edited by H. Gausterer and C. B. Lang (Springer-Verlag, Berlin, 1992), pp. 59-125.

[9] A. L. Talapov, and H. W. J. Blöte, J. Phys. A **29**, 5727 (1996).

[10] A. D. Bruce and N. B. Wilding, Phys. Rev. Lett. **68**, 193 (1992); N. B. Wilding and A. D. Bruce, J. Phys. Condens. Matter **4**, 3087 (1992).

[11] A. Rotenberg, J. Chem. Phys. **43**, 1198 (1965); D. Levesque, Physica **32**, 1985 (1966); B. J. Alder, D. A. Young, and M. A. Mark, J. Chem. Phys. **56**, 3013 (1972); I. B. Schrodt and K. D. Luks, *ibid.* **57**, 200 (1972).

[12] J. A. Barker and D. Henderson, Rev. Mod. Phys. **48**, 587 (1976); D. Henderson, W. G. Madden, and D. D. Fitts, J. Chem. Phys. **64**, 5026 (1976); W. R. Smith and D. Henderson, J. Chem. Phys. **69**, 319 (1978); D. Henderson, O. H. Scalice, and W. R. Smith, *ibid.* **72**, 2431 (1980).

[13] G. A. Chapela, S. E. Martinez-Casas, and C. Varea, *ibid.*, **86**, 5683 (1987).

[14] L. Vega, E. de Miguel, L. F. Rull, G. Jackson, and I. A. McLure, J. Chem. Phys. **96**, 2296 (1992).

[15] A. L. Benavides, J. Alejandre, and F. Del Rio, Molec. Phys. **74**, 321 (1991).

[16] G. Stell, K. C. Wu, and B. Larsen, Phys. Rev. Lett. **27**, 1369 (1976); M. Rovere, R. Miniero, M. Parrinello, and M. P. Tosi, Phys. Chem. Liq. **9**, 11 (1979); H. L. Friedman and B. Larsen, J. Chem. Phys. **70**, 92 (1979); W. Ebeling and M. Grigo, Ann. Physik. (Leipzig) **37**, 21 (1980).

[17] P. N. Vorontsov-Vel'yaminov and V. P. Chasovskikh, High Temp. (USSR) **13**, 1071 (1975); M. J. Gillan, Molec. Phys. **49**, 421 (1983); K. S. Pitzer and D. R. Schreiber, *ibid* **60**, 1067 (1987); J. P. Valleau, J. Chem. Phys. **95**, 584 (1991).

[18] A. Z. Panagiotopoulos, Fluid Phase Equilib. **76**, 97 (1992).

[19] J. M. Caillol, J. Chem. Phys. **102**, 100 (1994).

[20] G. Orkoulas and A. Z. Panagiotopoulos, J. Chem. Phys. **101**, 1452 (1994).

[21] M. E. Fisher and Y. Levin, Phys. Rev. Lett. **71**, 3826 (1993); M. E. Fisher, J. Stat. Phys. **75**, 1 (1994); X. Li, Y. Levin, and M. E. Fisher, Europhys. Lett. **26**, 683 (1994); M. E. Fisher, Y. Levin, and X. Li, J. Chem. Phys. **101**, 2273 (1994); Y. Levin and M. E. Fisher, Physica A **225**, 164 (1996).

[22] G. Stell, J. Stat. Phys. **78**, 197 (1995); Y. Zhou, S. Yeh, and G. Stell, J. Chem. Phys. **102**, 5785 (1995); S. Yeh, Y. Zhou, and G. Stell, J. Phys. Chem. **100**, 1415 (1995).

[23] K. S. Pitzer, Acc. Che. Res. **23**, 333 (1990); J. M. H. Levelt-Sengers and J. A. Given, Molec. Phys. **80**, 899 (1993).

[24] M. L. Japas and J. M. H. Levelt-Sengers, J. Phys. Chem. **94**, 5361 (1990).

[25] S. Wiegand, M. Kleemeier, J. M. Schröder, W. Schröer, and H. Weingärtner, Int. J. Thermo. **15**, 1045 (1994).

[26] K. S. Pitzer, M. C. P. de Lima, and D. R. Schreiber, J. Phys. Chem. **89**, 1854 (1985); R. R. Singh and K. S. Pitzer, J. Am. Chem. Soc. **110**, 8723 (1988); J. Chem Phys. **92**, 6775 (1990).

[27] K. C. Zang, M. E. Briggs, R. W. Gammon, and J. M. H. Levelt Sengers, J. Chem. Phys. **97**, 8692 (1992).

[28] P. Chieux, and M. J. Sienko, J. Chem. Phys. **53**, 566 (1970).

[29] T. Narayanan, and K. S. Pitzer, Phys. Rev. Lett. **73**, 3002 (1994); J. Phys. Chem. **98**, 9170 (1994); J. Chem. Phys. **102**, 8118 (1995).

[30] W. Schröer, M. Kleemeier, M. Plikat, V. Weiss, and S. Wiegand, J. Phys.: Condens. Matter **8**, 9312 (1996).

[31] S. Wiegand, J. M. H. Levelt Sengers, K. J. Zhang, M. E. Briggs, and R. W. Gammon, J. Chem. Phys. **106**, 2777 (1997).

[32] Z. W. Salsburg, J. D. Jacobson, W. Fickett, and W. W. Wood, J. Chem. Phys. **30**, 65 (1959); D. A. Chesnut and Z. W. Salsburg, *ibid.* **38**, 2861 (1963); I. R. McDonald and K. Singer, *ibid.* **47**, 4766 (1967); J. P. Valleau, and D. N. Card, *ibid.* **57**, 5457 (1972).

[33] A. M. Ferrenberg and R. H. Swendsen, Phys. Rev. Lett. **63**, 1195 (1989).

[34] T. L. Hill, *Thermodynamics of small systems, Parts I and II* (Dover, New York, 1962).

[35] W. W. Wood, J. Chem. Phys. **48**, 415 (1968).

[36] K. Binder, Z. Phys. B **43**, 119 (1981).

[37] B. A. Berg and T. Neuhaus, Phys. Lett. B **267**, 249 (1991); Phys. Rev. Lett. **68**, 9 (1992).

[38] J. Lee, Phys. Rev. Lett. **71**, 211 (1993).

[39] A. P. Lyubartev, A. A. Martsinovski, S. V. Shevkunov, and P. N. Vorontsov-Vel'yaminov, J. Chem. Phys. **96**, 1776 (1992).

[40] E. Marinari, and G. Parisi, Europhys. Lett. **19**, 451 (1992).

[41] A. E. Ferdinand, and M. E. Fisher, Phys. Rev. **185**, 832 (1969); M. E. Fisher and M. N. Barber, Phys. Rev. Lett. **28**, 1516 (1972).

[42] J. J. Rehr and D. N. Mermin, Phys. Rev. A **8**, 472 (1973).

[43] B. Widom and J. S. Rowlinson, J. Chem. Phys. **52**, 1670 (1970).

[44] D. N. Mermin, Phys. Rev. Lett. **26**, 169 (1970); *ibid.* **26**, 957 (1971); J. J. Rehr and N. D. Mermin, Phys. Rev. A **7**, 379 (1973).

[45] S. Jüngst, B. Knuth, and F. Hensel, Phys. Rev. Lett. **55**, 2160 (1985).

[46] A. D. Bruce, J. Phys. C: Solid State Phys. **14**, 3667 (1981).

[47] T_c for the three-dimensional Ising model is not known exactly. However, numerical calculations give T_c to a high accuracy, see references 7 and 9 for instance.

[48] R. Hilfer, and N. B. Wilding, J. Phys. A **28**, L281 (1995).

[49] G. E. Norman, and V. S. Filinov, High Temp. (USSR) **7**, 216 (1969).

[50] N. B. Wilding, Phys. Rev. E **52**, 602 (1995).

[51] J. V. Sengers and J. N. H. Levelt-Sengers, Ann. Rev. Phys. Chem. **37**, 189 (1986).

[52] A. J. Liu, and M. E. Fisher, Physica A **156**, 35 (1989).

[53] C. Borgs and R. Kotecky, J. Stat. Phys. **61**, 79 (1990); Phys. Rev. Lett. **68**, 1734 (1992).

[54] N. V. Brilliantov and J. P. Valleau, J. Chem. Phys. **108**, 1115 (1998); *ibid.* **108**, 1123 (1998).

[55] E. Luijten, H. W. J. Blöte, and K. Binder, Phys. Rev. E **54**, 4626 (1996).

[56] M. A. Anisimov, A. A. Povodyrev, V. D. Kulikov, and J. V. Sengers, Phys. Rev. Lett. **75**, 3146 (1995).

[57] Y. B. Melnichenko, M. A. Anisimov, A. A. Povodyrev, G. D. Wignall, J. V. Sengers, and W. A. Van Hook, Phys. Rev. Lett. **79**, 5266 (1997).

[58] S. W. De Leeuw, J. W. Perram, and E. R. Smith, Proc. R. Soc. London A **373**, 27 (1980); *ibid.* **373**, 57 (1980); D. M. Heyes, J. Chem. Phys. **74**, 1924 (1981); D. J. Adams, *ibid*. **78**, 1585 (1983).

[59] J. M. Caillol, D. Levesque, and J. J. Weis, Phys. Rev. Lett. **77**, 4039 (1996); J. Chem. Phys. **107**, 1565 (1997).

[60] J. M. Caillol, J. Chem. Phys.**99**, 8953 (1993).

[61] M. N. Barber , in *Phase Transitions and Critical Phenomena*, edited by C. Domb and J. L. Lebowitz (Academic, New York, 1983), Vol. 8, pp. 145-266.

[62] M. Müller, and N. B. Wilding, Phys. Rev. E **51**, 2079 (1995).

[63] R.C. Reid, J.M. Prausnitz and T.K. Sherwood, "*The Properties of Gases and Liquids,"* 3d edition (McGraw-Hill, New York 1977).

[64] N. B. Wilding and K. Binder, Physica A **231**, 439 (1996).

[65] J. Valleau, and G. Torrie, J. Chem. Phys. **108**, 5169 (1998).

[66] V. L. Ginzburg, Sov. Phys. Solid State **2**, 1824 (1960).

[67] R. J. F. Leote de Carvalho, and R. Evans, J. Phys. Condens. Matter **7**, 575 (1995).

[68] M. E. Fisher, J. Phys. Condens. Matter **8**, 9103 (1996).

[69] B. P. Lee, and M. E. Fisher, Phys. Rev. Lett **76**, 2906 (1996); Europhys. Lett. **39**, 611 (1997).

[70] M. E. Fisher, and B. P. Lee, Phys. Rev. Lett. **77**, 3561 (1996).

TABLE I Critical point parameters at the limit of infinite system size for the fluids studied in this work. All quantities are made dimensionless as discussed in section II. Statistical uncertainties are shown in parentheses, in units of the last decimal point reported for the corresponding quantity. The value of r was obtained from the limiting slope of the coexistence curve in the μ-K plane.

Fluid	T_c	ρ_c	P_c	$Z_c = \frac{P_c}{\rho_c T_c}$	μ_c/T_c	s	r
SW (λ=1.5)	1.2180(2)	0.310(1)	0.095(1)	0.252(3)	-2.9576(2)	-0.025(4)	-4.8(2)
SW (λ=3)	9.87(1)	0.257(1)	0.84(1)	0.332(4)	-2.8464(3)	-0.005(1)	-29.2(1)
RPM	0.0490(3)	0.070(5)	$8.2(3)\cdot10^{-5}$	0.024(4)	-27.27(1)	-1.5(1)	-0.62(2)

FIGURE CAPTIONS

FIG. 1 Order parameter probability distribution $P_L(x)$ for the λ=1.5 square-well fluid. The data have been obtained for an L=8 system size at T=1.220, and μ=-2.9518. The solid line corresponds to the universal Ising distribution $P^*_M(x)$, where $x=AL^{\beta/\nu}\delta M$. The nonuniversal scale factor A has been chosen so that the distributions have unit variance.

FIG. 2 Critical temperature (a) and density (b) scaling with system size for the square-well fluid with λ=3. Solid lines represent a least squares fit to the data.

FIG. 3 Coexistence curve of the square-well fluid with λ=1.5. Open symbols represent grand canonical Monte Carlo results of this work. (O): L=6; (◊): L=8; (Δ): L=12; (□): L=15. (●): critical point estimate of this work. (■): Vega *et al.* (1992), Gibbs ensemble Monte Carlo. Statistical uncertainties of the results from this work do not exceed the symbol sizes.

FIG. 4 Coexistence curve of the square-well fluid with λ=3. Open symbols represent grand canonical Monte Carlo results of this work. (O): L=6; (◊): L=8; (Δ): L=12; (□): L=15. (●): critical point estimate of this work. (■): Benavides *et al.* (1991), molecular dynamics.

FIG. 5 Temperature dependence of the vapor pressure for the λ=1.5 square-well fluid. (O): this work. (■): Brilliantov and Valleau, (1998). Simulation uncertainties are smaller than the symbol size.

FIG. 6 Temperature dependence of the vapor pressure for the λ=3 square-well fluid. Simulation uncertainties are smaller than the symbol size.

FIG. 7 Order parameter probability distribution for the restricted primitive model. (O): L=14, T=0.05024, μ=-26.513. (——): $P^*_M(x)$.

FIG. 8 Critical temperature (a) and density (b) scaling scaling with system size for the restricted primitive model. (O): this work. (□): Caillol *et al*. (1997).

FIG. 9 Coexistence curve for the restricted primitive model. (●): grand canonical Monte Carlo results of this work. (■): critical point estimate of Caillol *et al.* (1997). (□): Panagiotopoulos (1992). (Δ): Caillol (1993). (◊): Orkoulas and Panagiotopoulos (1994).

FIG. 10 Temperature dependence of the vapor pressure for the restricted primitive model. Statistical uncertainties are visible only for the critical pressure. For the other points, statistical uncertainties are smaller than the symbol size. The larger uncertainties for P_c result from the uncertainty in T_c.

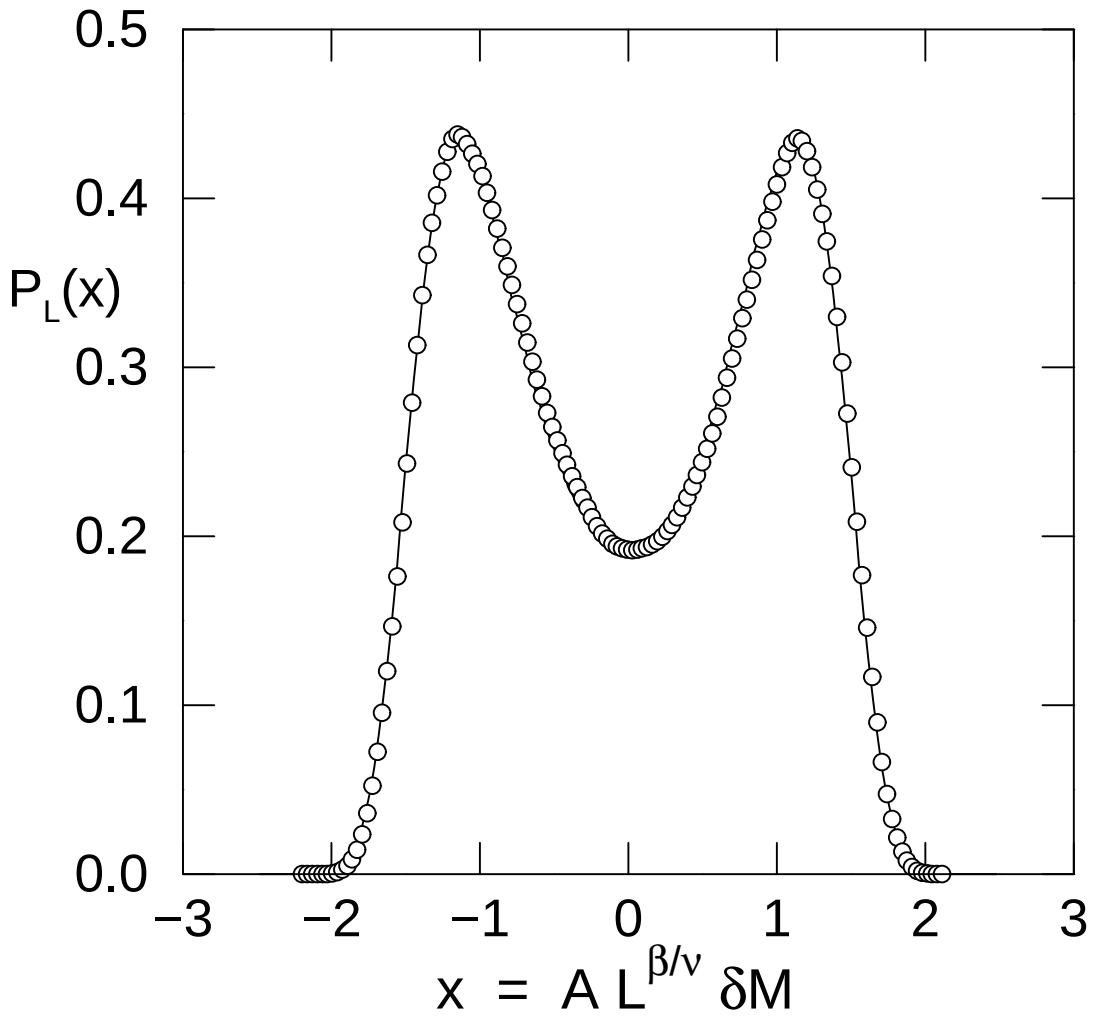

GO and AZP FIG. 1

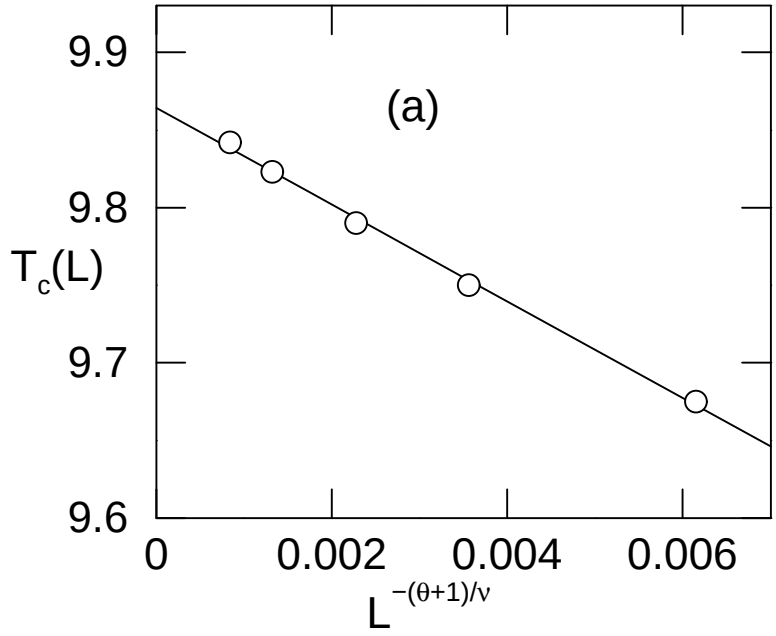

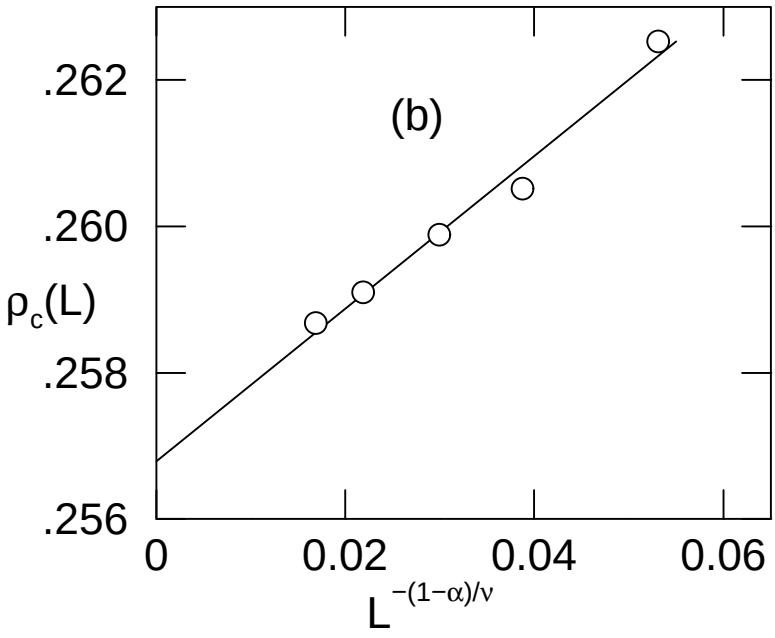

GO and AZP, FIG. 2

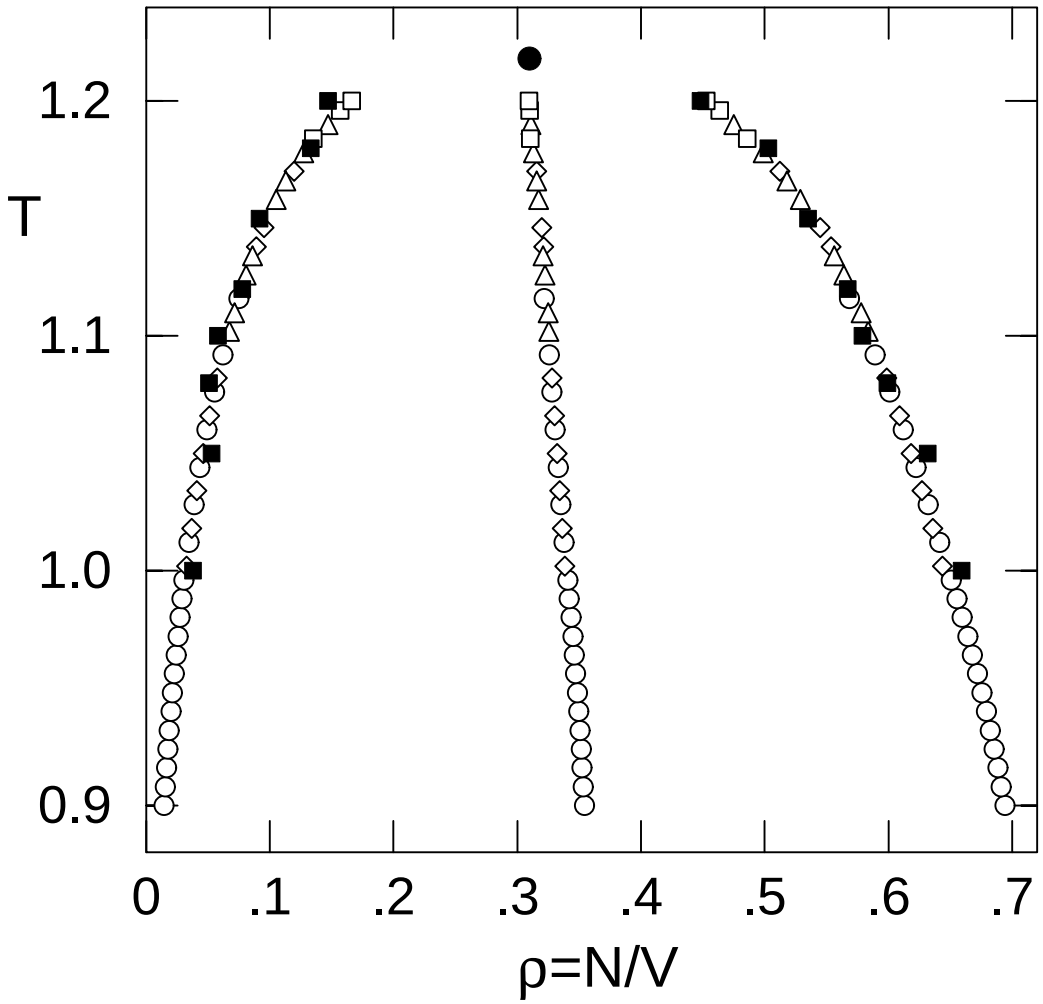

GO and AZP, FIG. 3

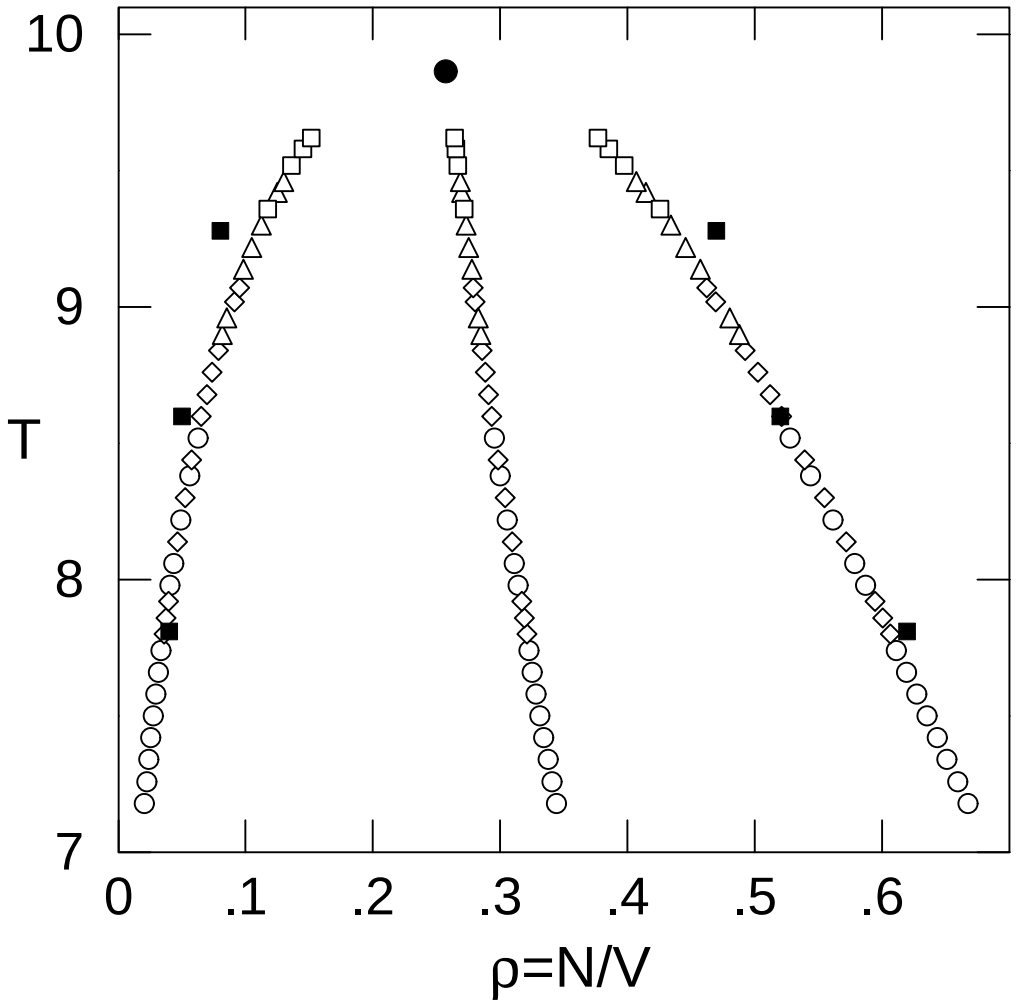

GO and AZP, FIG. 4

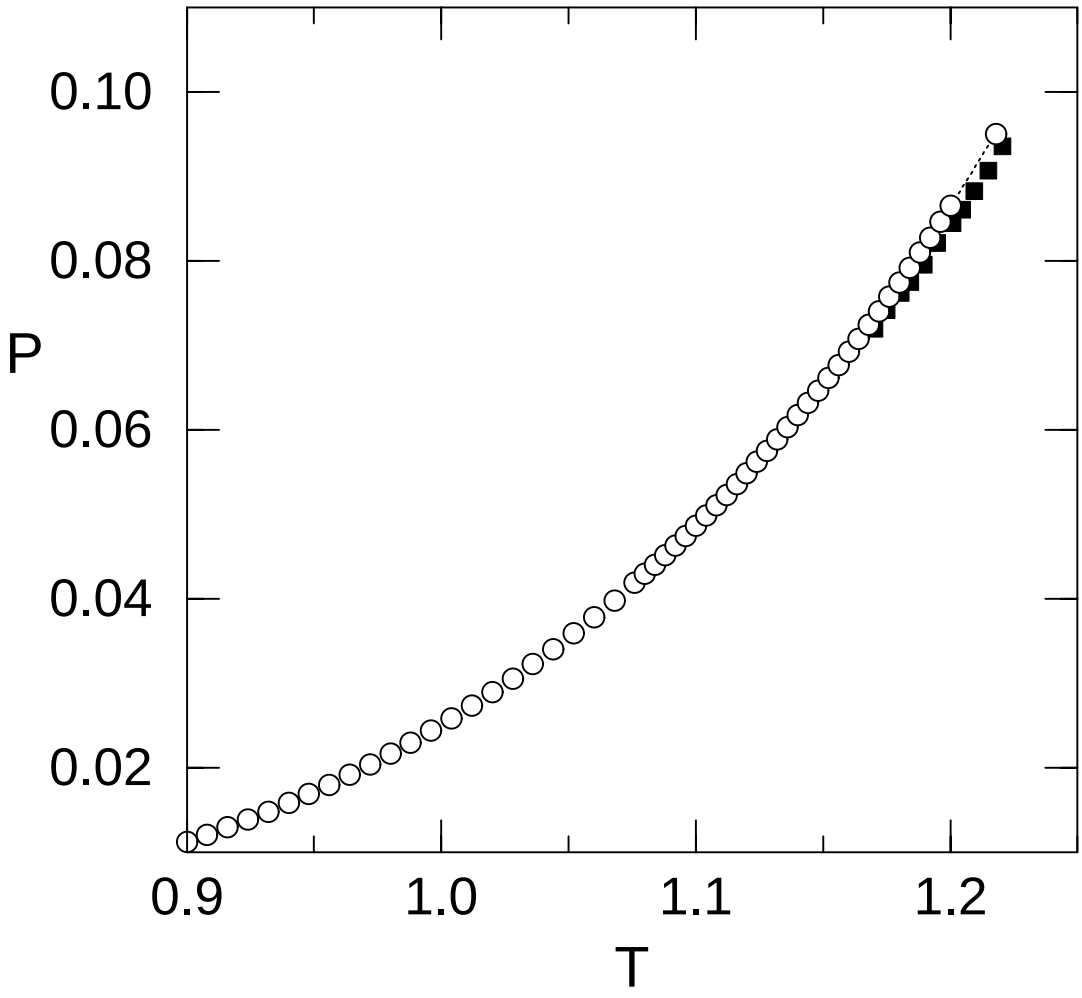

GO and AZP, FIG. 5

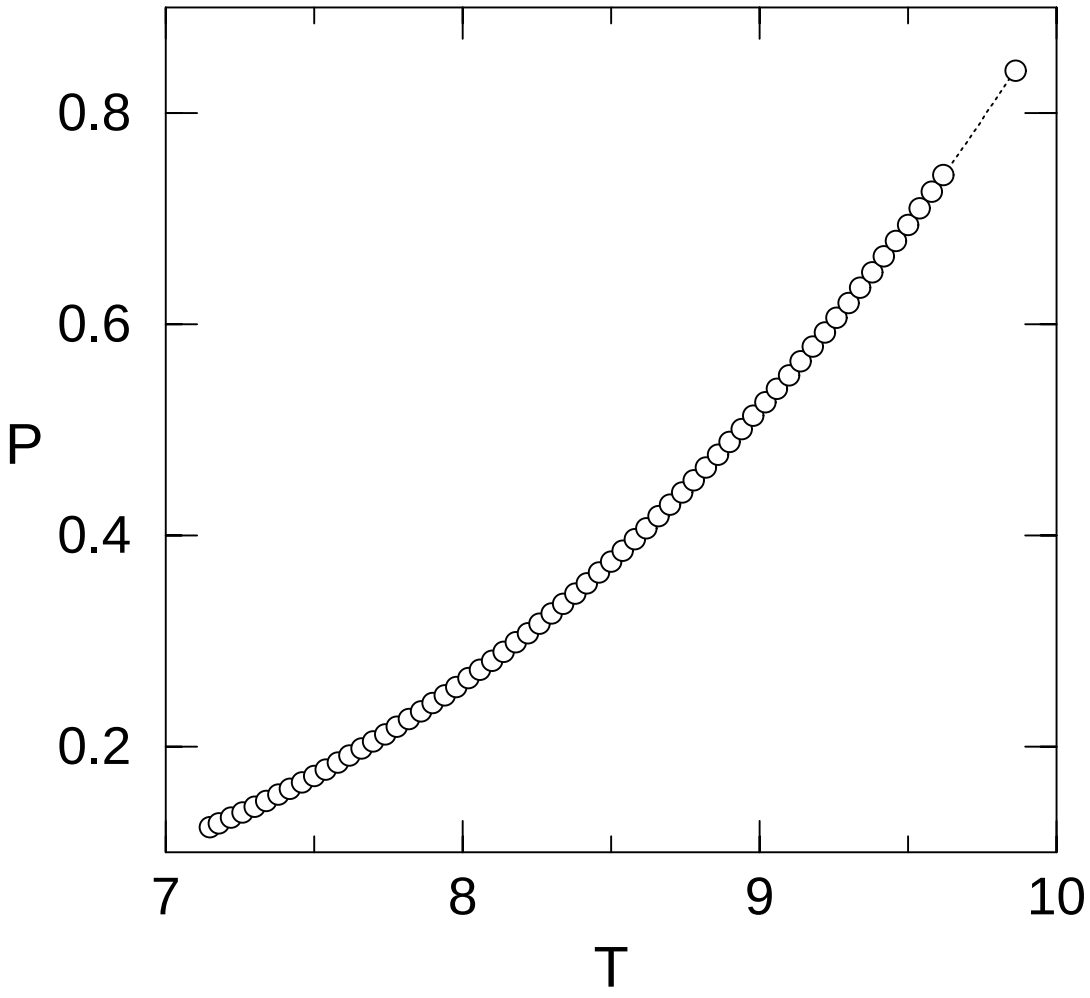

GO and AZP, FIG. 6

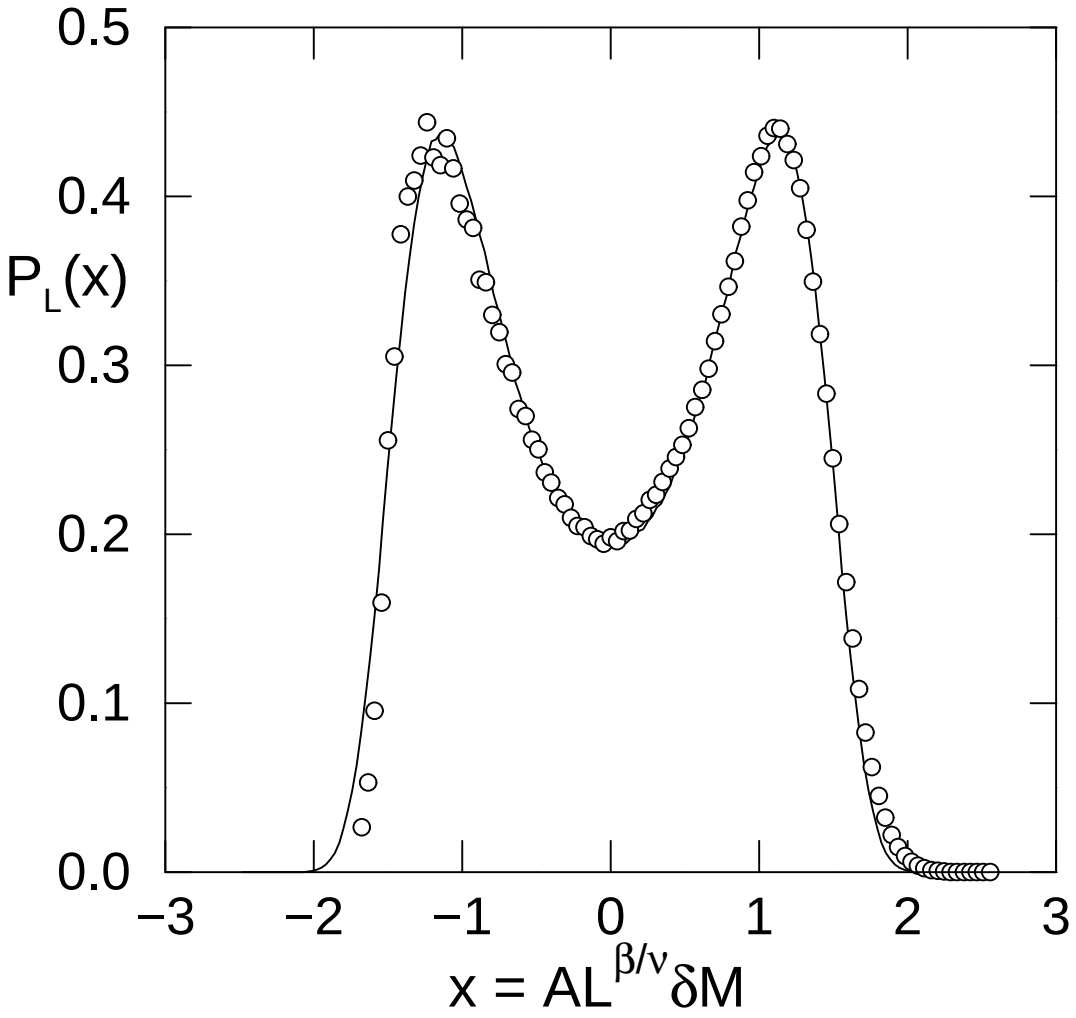

GO and AZP, FIG. 7

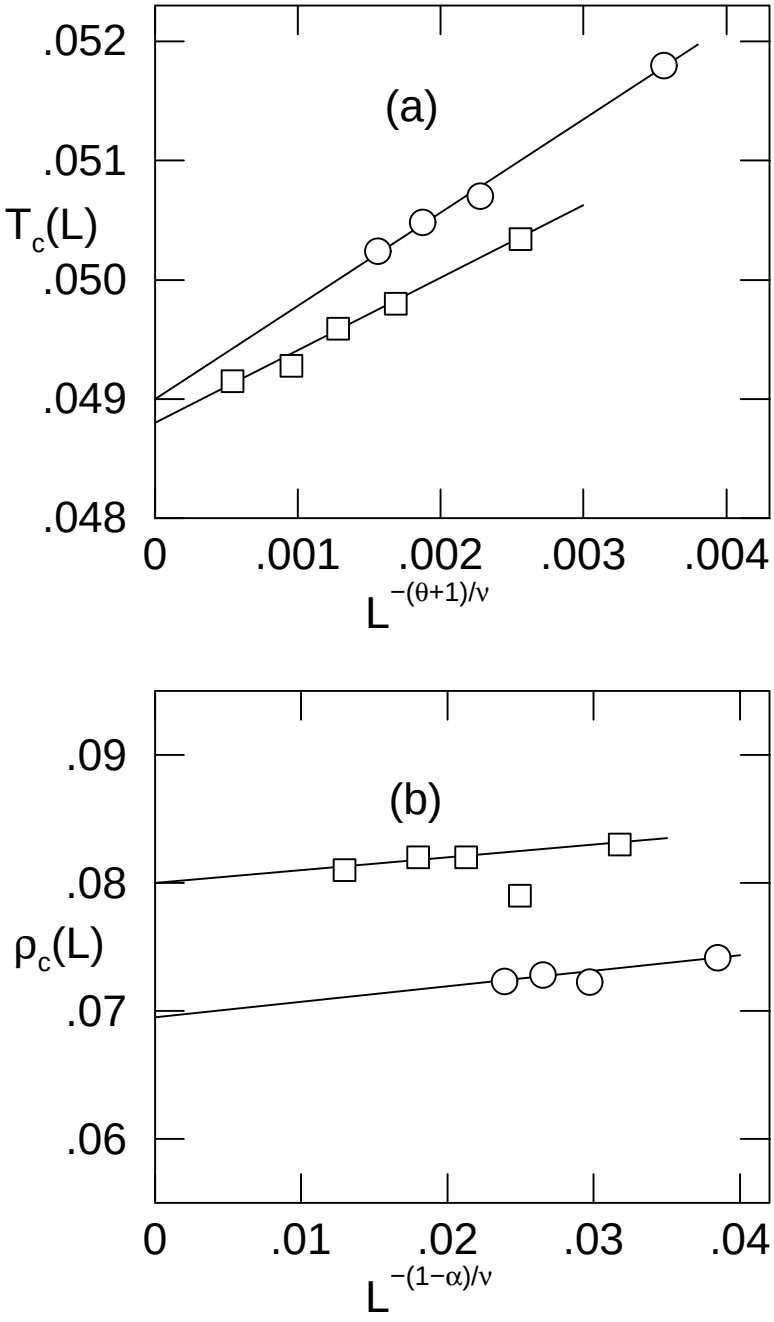

GO and AZP, FIG. 8

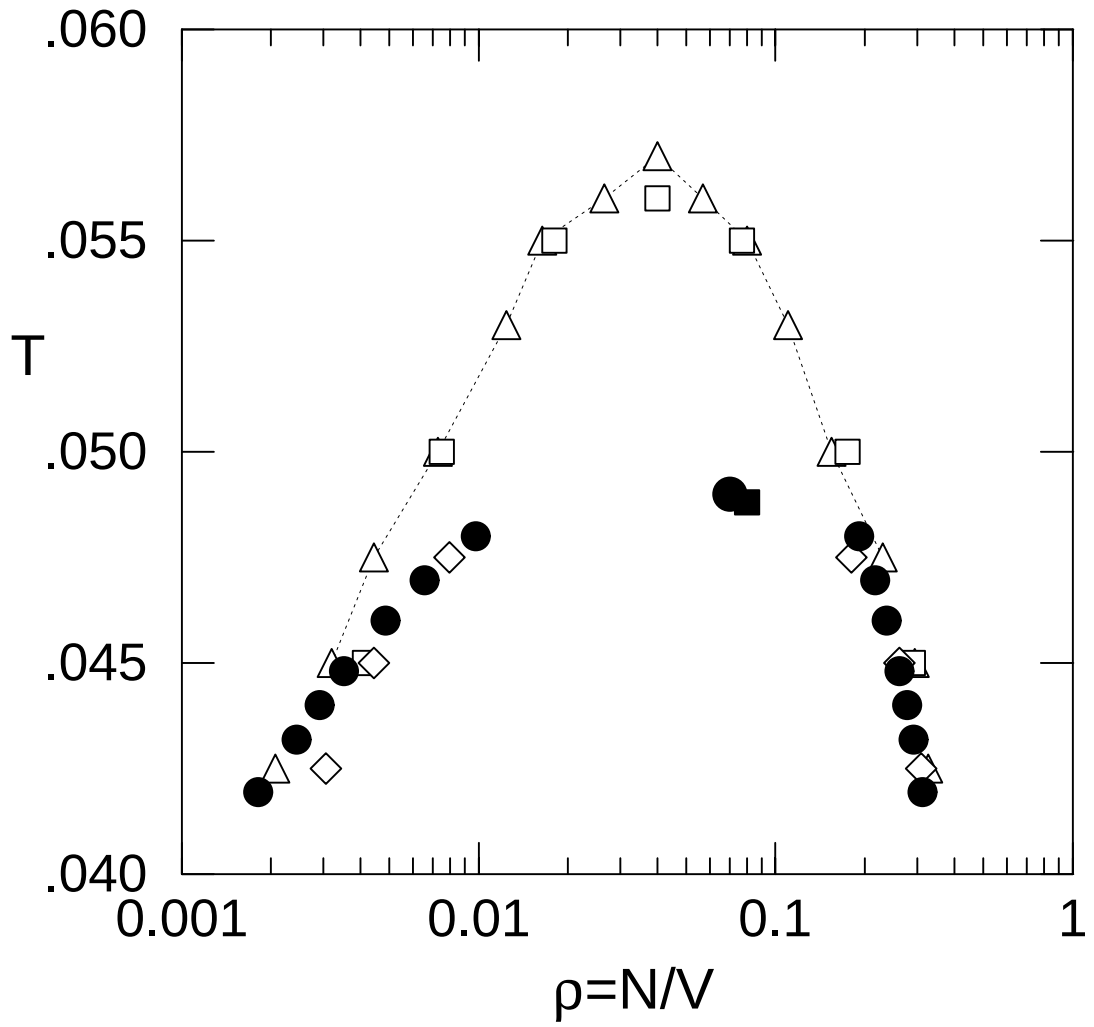

GO and AZP, FIG. 9

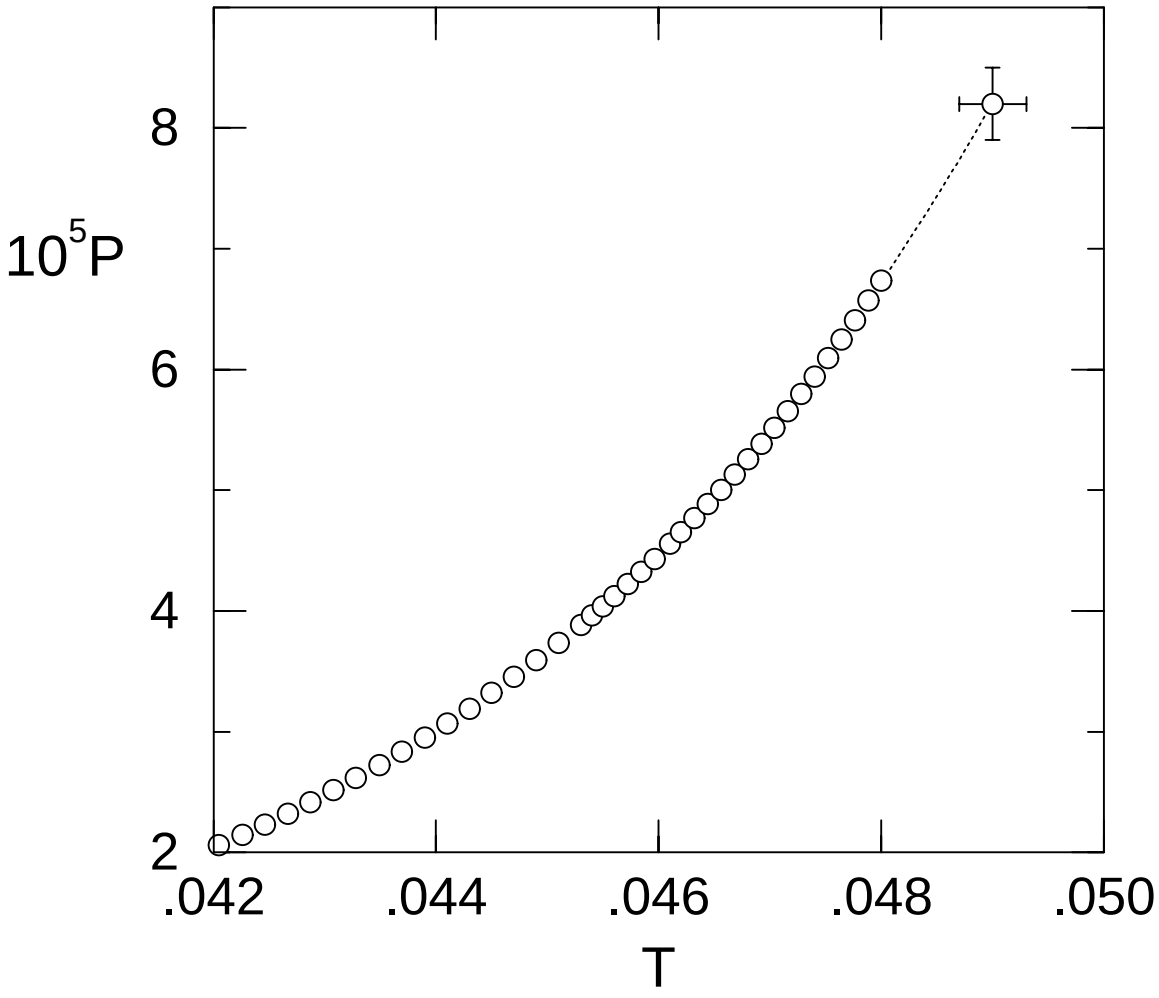

GO and AZP, FIG. 10